PARAMETER MATCHING CHARACTERISTICS OF HEAVY-DUTY CRAWLER VEHICLE AND ITS DRIVING MOTOR

Tiangang PEI[1], Bijuan YAN[1]*, Hao SU[1], Yong SONG[1]

To further improve its' working performance, it is necessary to precisely match the tracked vehicle-drive motor parameters. Based on the theoretical analysis of the main parameters of the crawler driving motor, a motor control system model is built using Matlab/Simulink. At the same time, a three-dimensional model of the crawler vehicle is created using RecurDyn. At last, a joint vehicle-motor simulation model is established in Matlab. Taking a certain type of heavy-duty crawler vehicle as an example, its parameter matching characteristics are analyzed and discussed under three typical operating conditions. The results show that the driving speeds eventually reach near the set value under three operating conditions, after that the vehicle starts to travel at a constant speed (v_1 = 8 m/min, v_2 = 5 m/min and v_3 = 3 m/min). In addition, the load torque fluctuates around the analytical torque and the displacements appear a linear increase after the requirements has been reached. In summary, the established crawler vehicle-motor coupling model in different working conditions can control the motor speed effectively, and meet the actual working requirements of the vehicle. The results can provide theoretical support for the selection of drive motor parameters for the tracked vehicles, and can also provide some reference for the design of heavy-duty vehicles.

Keywords: Crawler vehicle; Driving motor; Parameter matching; typical operating conditions.

[1]School of Mechanical Engineering College, Taiyuan University of Science and Technology, China, e-mail: peitiangang@126.com. *Corresponding Author.

1.Intorduction

Heavy-duty crawler vehicles play an irreplaceable role in engineering construction [1-3]. Driving motors are usually regarded as the core component of the crawler walking system. The reasonable parameter matching between the crawler vehicles and driving motors are important to improve the control accuracy, power and economy performances as well as other performances such as the acceleration and deceleration of the whole vehicles [4].

To address the above problems, the researchers have done many efforts. For example, WANG et al. designed a special robust controller for the tracked vehicle M113 and verified the performance of the controller [5]. Cao used a novel direct-torque control technique, and the effectiveness and robustness of the proposed control approach was verified [6]. Niu proposed a novel model predictive control for a three-phase permanent magnet synchronous motor (PMSM) with enhanced robustness against parameter variation and higher current control precision [7]. Sun et al. used RecurDyn and Matlab/Simulink to jointly simulate the whole vehicle travelling device and proposed a kind of torque control strategy [8]. The literature [9] presented a control strategy for induction motor which optimized both efficiency and torque response under the transient and steady state. Chen Shuyong et al. used RecurDyn, Matlab/Simulink and vector control to model and simulate the motor system and predict the motion performance of the studied vehicle [10]. Xiao established the stochastic dynamic model of vehicle-track-bridge (VTB) [11]. In addition, the vertical dynamic interaction between a travelling railway vehicle and a slab track is simulated in the time domain by using an extended state-space vector approach [12]. Zhan et al. analyzed dynamic stability of the electric crawler in the typical working environments [13]. Wang et al. developed a kinematic model for a high-speed tracked vehicle, considering the effect of steering friction and track sliding on the vehicle [14]. The steering control strategies considering the slip which can improve steering control accuracy was verified through simulations and experiments in the literature [15].

From the above literature review, it can be seen that most of the current research are focused on military high-speed tracked vehicles, while there is less research on heavy-duty mining vehicles. Mining vehicles are an important ground or underground equipment for the transportation of minerals. Now, higher requirements on their power and economy performance have been proposed. To tackle the challenge of performance parameter matching heavy-duty equipment on

the mining, this paper established the analytical model of the driving motor parameters, and after that the motor's speed control model is built using Matlab/Simulink software. Then, the dynamics model of the crawler travelling mechanism is conducted in RecurDyn software. At last, the control model and dynamic model are co-simulated to study the parameters matching characteristics of vehicle-motor under typical working conditions. The results of this paper could provide the helpful reference for the designs of various vehicles.

1 Analytical model of the driving motor

The related parameters of driving motor mainly include rated and maximum power, speed, torque.

1.1 Rated power P_e and maximum power P_{max}

The rated power P_e at the maximum travelling speed is calculated as [16]:

$$P_e \geq \frac{1}{2\times 3600\eta_{ch}\eta_x}(fG+\frac{C_w A v_{\max}^2}{21.15})v_{\max} \tag{1}$$

where η_{ch} is transmission efficiency between the motor to driving wheel; η_x is Crawler travel unit efficiency; f is the rolling resistance coefficient; G is the vehicle weight; v_{max} is the maximum travelling speed; C_w is the Air drag coefficient and A is the positive projected area of the vehicle.

The crawler vehicles are often steered by skid steering whereby the tracks on either side of the vehicle are rotated at different speeds. Here, the maximum speed of the outer track is required to be no less than the maximum speed of the vehicle. Therefore, the maximum power $P_{\max 1}$ at this time is gotten as [17].

$$P_{\max 1}=\frac{k_p F_w v_w}{3600\eta_{ch}\eta_x}=\frac{k_p\left(0.5fG+\dfrac{0.25\mu GL}{B}\right)v_w}{3600\eta_{ch}\eta_x}=\frac{k_p\left(0.5fG+\dfrac{0.25\mu_{\max}GL}{0.925B+\dfrac{0.15v_a^2}{3.6^2 a_c}}\right)v_w}{3600\eta_{ch}\eta_x} \tag{2}$$

where k_p is the motor overload ratio; F_w is the tractive force of the outer track; v_w is the travelling speed of the outer track; L is ground contact length of crawler; v_a is the forward velocity; a_c is the lateral acceleration; B is the Track centre distance; μ is the steering friction coefficient; μ_{max} is the maximum steering friction coefficient (for a relative turning radius ρ=0.5).

In addition, when the vehicle need to climb a slope, it is affected by slope resistance, air resistance, rolling and other resistance. At this point the maximum power $P_{\max 2}$ is given by:

$$P_{\max 2}=\frac{\left(fG\cos\alpha_{p\max}+G\sin\alpha_{p\max}+\frac{C_wAv_{\max}^2}{21.15}\right)\cdot v_{\max}}{3600\eta_{ch}\eta_x} \tag{3}$$

where $\alpha_{p\max}$ is the maximum climbing angle. Therefore, in this paper, the maximum power of the driving motor is chosen by $P_{\max}=\max\{P_{\max 1}、P_{\max 2}\}$.

1.2 Rated speed n_e and maximum speed $n_{\max}$

According to the external characteristics of the motor [18-19], the relationship between its maximum speed $n_{\max}$ and rated speed n_e is described as:

$$n_e=\frac{n_{\max}}{\beta} \tag{4}$$

where β is extended constant power area of motor.

1.3 Rated torque T_e and maximum torque $T_{\max}$

The rated torque of the motor T_e can be calculated from its rated power. The maximum torque $T_{\max}$ is gotten in two cases [20]. The first is considered for driving on a 1:10 slope, where the maximum value of the one-sided power factor $D_{x\max}$ is expressed as:

$$D_{x\max}=\sin(\arctan 10\%)+f\cos(\arctan 10\%) \tag{5}$$

The second is considered for one-sided track travel on a flat road with two-sided power steering, at this time, the maximum value of the power factor $D_{w\max}$ is described as

$$D_{w\max}=f+\frac{\mu_0 L}{2B} \tag{6}$$

where μ_0 is the unilateral power steering friction coefficient.

Therefore, the maximum torque $T_{\max}$ for tracked vehicles is gotten as:

$$T_{\max}=\frac{F_{\max}\cdot r}{i\eta_{ch}\eta_x}=\frac{s_q\left(D_{\max}\cdot G/2\right)\cdot r}{i\eta_{ch}\eta_x}=\frac{s_q D_{\max}\cdot G\cdot r}{2i\eta_{ch}\eta_x} \tag{7}$$

where $D_{\max}=\max\{D_{x\max}、D_{w\max}\}$; r is the working radius of the driving wheel; i is travel drive motor gearbox ratio and s_q is the Start-up factor.

2 Coupled modeling of tracked vehicle and motor

2.1 Motor speed control system model

Three-phase asynchronous motors are used in the crawler vehicle. It is difficult to establish the mathematical model of driving motors owing to their highly strongly coupled characteristics. Here, the motors are modelled using the

Clark and Park transform. The equations for the induction motor are written as:

$$\begin{aligned}
\frac{d\omega}{dt} &= \frac{n_p^2 L_m}{JL_r}\left(i_{sq}\psi_{rd} - i_{sd}\psi_{rq}\right) - \frac{n_p}{J}T_L \\
\frac{d\psi_{rd}}{dt} &= -\frac{1}{T_r}\psi_{rd} + (\omega_n - \omega)\psi_{rq} + \frac{L_m}{T_r}i_{sd} \\
\frac{d\psi_{rq}}{dt} &= -\frac{1}{T_r}\psi_{rq} + (\omega_n - \omega)\psi_{rd} + \frac{L_m}{T_r}i_{sq} \\
\frac{di_{sd}}{dt} &= \frac{L_m}{\sigma L_s L_r T_r}\psi_{rd} + \frac{L_m}{\sigma L_s L_r}\omega\psi_{rq} - \frac{R_s L_r^2 + R_r L_m^2}{\sigma L_s L_r^2}i_{sd} + \omega_n i_{sq} + \frac{u_{sd}}{\sigma L_s} \\
\frac{di_{sq}}{dt} &= \frac{L_m}{\sigma L_s L_r T_r}\psi_{rq} + \frac{L_m}{\sigma L_s L_r}\omega\psi_{rd} - \frac{R_s L_r^2 + R_r L_m^2}{\sigma L_s L_r^2}i_{sq} + \omega_n i_{sd} + \frac{u_{sq}}{\sigma L_s}
\end{aligned} \tag{8}$$

where ω is the rotor speed, $\omega_n=2\pi f$ is the magnetic field rotation speed, n_p is pole pair, L_s is the stator winding inductance, L_r is the rotor winding inductance, L_m is the mutual inductance between the stator and rotor windings, T_L is the load torque, J is the motor moment of inertia, R_s the flux stator resistance, R_r is the rotor winding resistance, i_{sd}, i_{sq} are the rotor winding current, Ψ_{sd}, Ψ_{sq} are the stator fluxes, u_{sd}, u_{sq} are the stator voltages, $\sigma=1-(L_m^2/\ L_r L_s)$ is the motor magnetic leakage coefficient, $T_r= L_r / R_r$ is the rotor electromagnetic time constant.

According to equation (8), a motor control system model is built using Matlab/Simulink, which is shown in Fig. 1. The input and output in the Fig. 1 are the actual and theoretical motor speed, respectively.

The control module of the motor includes asynchronous motor module, motor measurement module, coordinate transformation module, and various corresponding adjustment module. In the Simulink software, the motor control simulation model is built and the related parameters of the motor module are set. At the same time, the speed regulation system is established. The speed regulation system of the motor includes triple-phase asynchronous motor, current hysteresis tracking PWM generator, speed regulation module, power supply, and control unit.

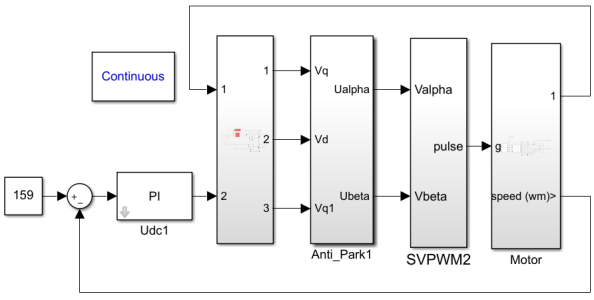

Fig. 1 Motor speed control system

2.2 Tracked vehicle model

The model of the heavy tracked vehicle is created in RecurDyn. The model consists of a simplified vehicle body and a travelling mechanism.

The dynamics model of the travelling mechanism includes the Caterpillar chassis and the crawler chains on both sides. The Caterpillar chassis system includes suspension, driving wheel and so on. The crawler chain is composed of a closed loop structure connected by pin shafts at both ends. The three-dimensional Digital Mock-Up of the crawler vehicle are established by SolidWorks software and imported into RecurDyn software. Constraints and friction are added in RecurDyn, and simulation parameters are set. The adjacent crawler plates are connected by rotating pairs, and the attachment coefficient between crawler plates and soil is set to 0.6. Geometric parameters and constraints between other components are set to complete the dynamic modeling of the vehicle. The fixed coordinate system selected for model is the geometric center of the driving wheel.

2.3 Vehicle-motor coupling simulation model

According to 2.1 and 2.2, a joint vehicle-motor simulation model is established in Matlab, which is shown in Fig 2. The input of the crawler vehicle model in RecurDyn is set to the speed of the crawler driving wheels on both sides, the center of the drive wheels on both sides is selected as the reference coordinate system, and the output is the speed and displacement of the center of the driving wheels on both sides. The simulation files are output as '.m' files. And the Matlab/simulink control program is used as the main program for joint simulation. Considering that for heavy vehicles the independent motors are often used to drive for both sides of the tracks, and that the traction motors and drive systems are identical on both sides, the motors on both sides are controlled in the same way.

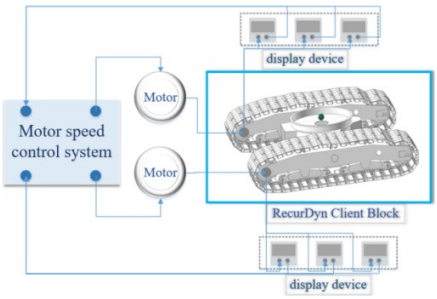

Fig. 2 Vehicle-motor simulation model

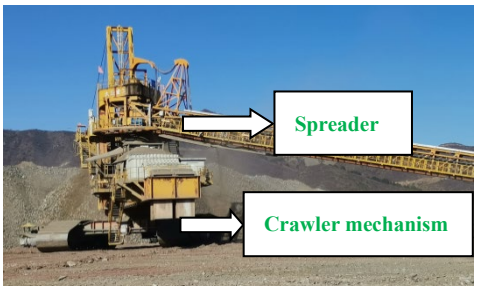

Fig. 3 Spreader structure diagram

3 Parameter matching characteristics in typical operating conditions

3.1 Crawler mechanism-motor parameters

Taking a certain type of spreader in China (as shown in Fig 3) as the research object, its maximum speed is 8 m/min, the maximum driving wheel speed is 0.159 rad/s and the maximum climbing gradient is 1:10. The basic parameters of the track mechanism are shown in Table 1.

Table 1

Basic parameters of the crawler mechanism

Parameter name	Numerical values
Transmission efficiency between motor and driving wheel η_{ch}	0.95
Crawler travel unit efficiency η_x	0.85
Rolling resistance coefficient f	0.2
Maximum wind speed borne by the spreader/m•s^{-1}	22
Air drag coefficient C_w	1.0
Track centre distance B/m	10
Ground contact length of crawler L/m	8.6
Start-up factor s_q	1.2
Extended constant power area of motor β	2.4
Travel drive motor gearbox ratio i	1 000

The calculation results of the drive motor are shown in Table 2.

Table 2

Drive motor matching parameters

Motor parameters	Matching values
Rated power P_e/kW	35.53
Maximum Power P_{max}/kW	75
Rated torque n_e/N•m	385
Maximum torque T_{max}/N•m	1 035
Maximum speed/rad•s^{-1}	159

3.2 Simulation analysis under typical operating conditions

The speeds, displacements and load torque (the driving wheel torque) of the crawler mechanism under three typical operating conditions including going straight along a flat road, turning (single-sided power, double-sided opposite power) and climbing a slope are analyzed, respectively. The simulation time is set to 10 s. The speed at which the spreader travels (the ideal speeds of the driving wheels) are set as v_1=8 m/min (0.159 rad/s), v_2=5 m/min (0.0 994 rad/s) and v_3=3 m/min (0.0 596 rad/s).

3.2.1 Going straight along a flat road

The simulation results when the tracked vehicles go straight along a flat road are shown in Fig 4. As can be seen from Fig 4(a) that the speeds of the driving wheels rapidly increase to a maximum value within 0.15s, where v_1 increases to 0.640 rad/s, v_2 reaches 0.628 rad/s and v_3 becomes 0.598 rad/s. Subsequently, v_1 decreases to 0.032 rad/s, v_2 decreases to 0.030 rad/s and v_3 decreases to 0.023 rad/s. What's more, the consuming time of reaching a minimum speed are t_{v1}= 0.39s, t_{v2}= 0.36s and t_{v3}=0.32s respectively. This phenomenon is due to the poor track tension pulley of the spreader as a heavy equipment, with less resistance and a sharp increase in speed during the initial speed-up phase, after that the tension pulley are tightened and the speed returns to normal. At the same time, the simulated speed-time relationship for the three different speeds is approximately linear from the lowest speed to 1.3 s. At this time, the driving wheel speed is in a state of uniform forward acceleration, and the speed fluctuates from 1.3 to 1.6 s. After that, it stabilizes around 0.159 rad/s(v_1), 0.0994 rad/s(v_2) and 0.0596 rad/s(v_3), indicating that the spreader starts to walk at the giving speed.

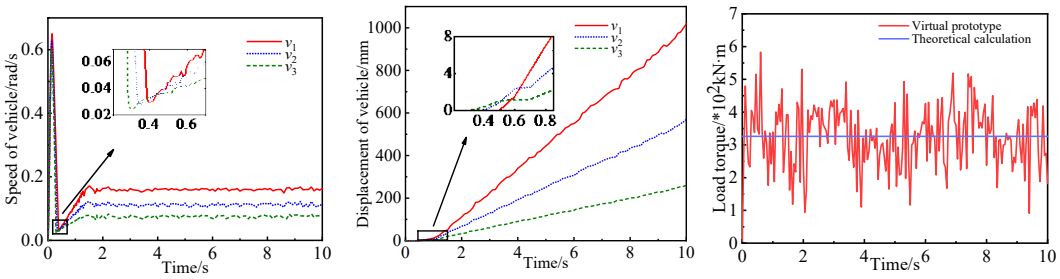

(a) Rotation speed-time (b) Displacement-time (c) Load torque-time

Fig. 4 The driving state under going straight along a flat road

At the same time, it can be seen from Fig 4(b) that the displacement variations are almost zero in the initial phase from 0 to 0.2 s. The displacement then increased slowly to 146 mm (v_1), 95 mm (v_2) and 65 mm (v_3) for the three different travel speeds. And the displacements increase approximately linearly after 1.3 s and from this time the vehicle moves at a constant speed. After the simulation finish for about 10s, the driving distances at three speeds are 1 015 mm(v_1), 563 mm(v_2) and 278 mm(v_3), respectively. After the crawler vehicle reaches a stable driving condition, the driving wheel torque is equal at different speeds. Verification is based on the maximum speed. Fig. 4(c) shows the load torque fluctuates around the analytical value in maximum speed. In the data, the maximum value is 582.92kN·m and the minimum value is 91.03kN·m.

3.2.2 Turning working conditions

(1) Single-sided power turning

The final speeds of one-sided driving are 0.159 rad/s (v_1), 0.0 994 rad/s (v_2) and 0.0 596 rad/s (v_3). As is shown in Fig 5(a), the speed variation of the driving wheels at the three different speeds follows the same trend as the speed profile when driving straight on a flat road. Taking v_1 as an example, the zero-power side ($v_{1\ r}$) which drives in the opposite direction of travel has the same trend as the power side ($v_{1\ f}$), but its speed is lower than that of the power side at the same moment, because the track structure is complex and the two sides are coupled to some extent, which affects the motion between the two sides. The speed of the zero-power side finally tends to stable around 0.047 rad/s, with a ratio of 3.4 between the power side and the zero-power side, and the speed of the zero-power side fluctuates much less. At the same time, it can be seen from Fig 5(b) that the bilaterally displacement variations of the tracked vehicle at three different travel speeds are basically the same as those of going straight. The distances at the end of calculation are 1,018 mm and 298 mm (v_1), 615 mm and 194 mm (v_2) and 313 mm and 105 mm (v_3), respectively. Fig. 5(c) shows the load torque fluctuates around the analytical value when the speed is maximum speed and the maximum value is 996.53kN·m, the minimum value is 90.39kN·m.

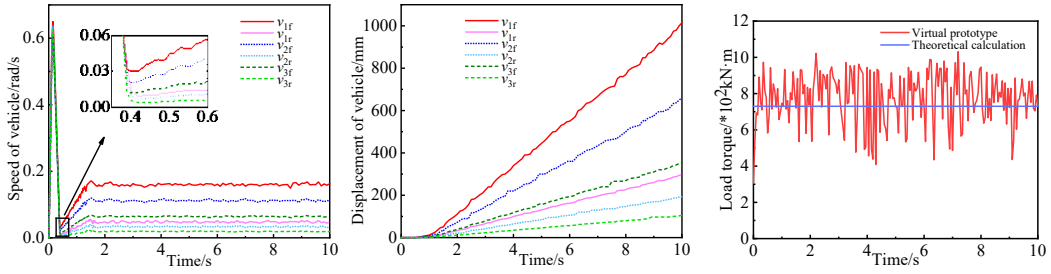

(a) Rotation speed-time (b) Displacement-time (c) Load torque-time

Fig. 5 The driving state under single-sided power turning

(2) Double-side powered turning

In this operating condition, the final speeds of the tracked vehicle driving wheels are set to be of equal magnitude and in opposite directions. As is shown in Fig. 6(a), when the reference speed v_c =0, the final speed is still around 0.159 rad/s for the example of v_1. For the three different speeds, the trend of the speed change on both sides is symmetrical along the time axis, the unilateral speed curve

is the same as speed curves of going straight, the bilateral speed curve contrasts in magnitude and the speed finally stabilizes around 0.159 rad/s (v_1), 0.0 994 rad/s (v_2) and 0.0 596 rad/s (v_3) respectively. Meanwhile, Fig. 6(b) shows that the magnitudes of bilateral displacements at different velocities are essentially equal. Fig. 6(c) shows the load torque fluctuates around the analytical value in maximum speed. The torque variation pattern is the same on both sides. In the data, the maximum value is 1026.46kN·m and the minimum value is 307.18kN·m. Comparing the torque values, the double-side powered turning is larger than going straight along a flat road, and the difference with single-sided power turning is within 5%.

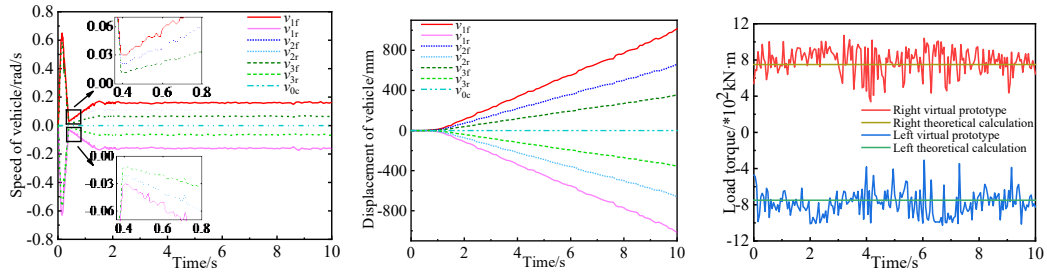

(a) Rotation speed-time (b) Displacement-time (c) Load torque-time

Fig. 6 The driving state under double-side powered turning

3.2.3 Climbing slope

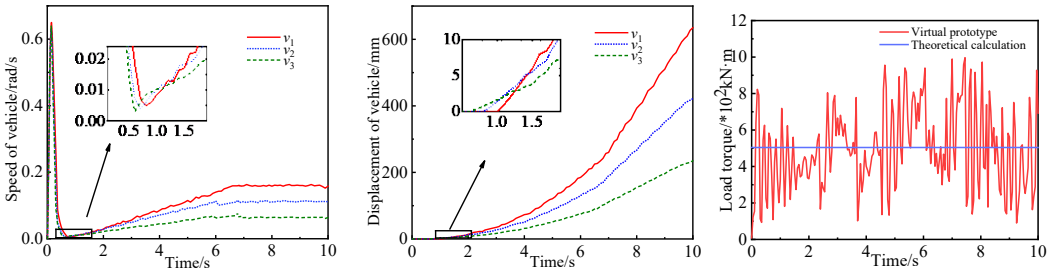

(a) Rotation speed-time (b) Displacement-time (c) Load torque-time

Fig. 7 The driving state under climbing slope

As is shown in Fig 7(a), the driving speed in 0-0.6 s is similar to that of going straight along a flat road, and basically shows a straight upward trend in the 0.6-6.6 s period, with the track in a state of uniform acceleration, and the drive

speed stabilizes around the requirements at 6.6 s, after which the vehicle is maintained in a state of uniform motion. The maximum travel distances in Fig 7(b) are 630 mm (v_1), 422 mm (v_2) and 235 mm (v_3), which are significantly lower than the final value of the displacements under the working condition of going straight in the flat road. Fig. 7(c) shows the load torque fluctuates around the analytical value in maximum speed and the maximum value is 1026.46kN·m, the minimum value is 307.18kN·m. The torque value is higher than that of the going straight along a flat road and lower than that of the turning working conditions.

At last, from Figs 4(a)-7(a), the drive speeds eventually reach near the set value under three operating conditions, after that the vehicle starts to travel at a constant speed. Figs 4(b)-7(b) show a linear increase in displacement after the requirements has been reached, indicating that the vehicle can travel steadily under these typical operating conditions. As shown in Figs 4(c)-7(c), when the crawler runs stably under typical operating conditions, the driving wheel torque fluctuates around the analytical value. In all typical operating conditions, the maximum torque is double-side powered turning and the minimum torque is going straight along the flat road. In summary, it can be seen that the established crawler vehicle-motor coupling model in different working conditions can control the motor speed effectively, and meet the actual working requirements of the vehicle. The parameters match between the vehicle and its driving motor is reasonable.

4. Conclusion

Taking a certain type of heavy-duty crawler vehicle as an example, its parameter matching characteristics are analyzed and discussed on the basis of coupled vehicle-drive motor modelling. The conclusions are summarized as follows:

(1) A coupled tracked vehicle-motor simulation model is established. In this case, the tracked vehicle model consists of a simplified body and a travelling mechanism. At the same time, a motor control model is built in Simulink software.

(2) The final speeds of the tracked vehicle after the motor speed regulation system meets the requirements under three typical operating conditions. Under the going straight and climbing conditions, the speed fluctuates around the requirements (v_1 = 0.159 rad/s, v_2 = 0.0 994 rad/s and v_3 = 0.0 596 rad/s) in the steady state. Under the unilateral power turning condition, the power side velocity

fluctuates at the requirements during steady state, with the ratio of zero power side to power side velocity around 3.4. In addition, when the vehicle turns with the condition of bilateral opposite power, the speeds of two tracks fluctuate around the requirements in steady state with equal velocities and opposite directions. The tracked vehicle driving wheel displacement increases steadily after the motor speed regulation in different working conditions, which meets the requirements. In the maximum speed condition, the torque fluctuates around the analytical value, which is in line with the actual situation.

The results can provide theoretical support for the selection of the crawler vehicles drive motor parameters, and can also provide some reference for the design of various heavy-duty vehicles.

Acknowledgements

The authors would like to thank the Nonlinear viscoelastic suspension for "off-road" vehicles under temperature-frequency coupling excitation Optimization strategy of ride comfort（SY2022044）and the Key Research and Development Program of Shanxi Province（202102010101010）for their support.

REFERENCES

[1] *M. A. Ghulam, S. M. ASCE, O. Jacek, B. Ahmed A. H. Mohamed and M. ASCE.* "Implementation of combined loading to calculate ground bearing pressure under crawler crane tracks". Journal of Construction Engineering and Management, **vol. 147**, no.7, July. 2021, pp. :04021051.

[2] *Y. Zhou* "Dynamics analysis of the static gantry structure of a double-tracked earth-moving machine". Tsinghua University, 2013 pp. 15-30.

[3] *P. F. He, J. Li, D. Q. Zhang and S. Wan*. "Optimisation of the harvesting time of rice in moist and non-moist dispersed fields". Biosystems Engineering, **vol. 170**, June. 2018, pp. 12-23.

[4] *C. Jakub, A. D. Piotr and K. Michael*. "On the energy losses due to tracks vibrations in rubber track crawler vehicles". Archives of Civil and Mechanical Engineering, **vol. 21**, no. 2 March 2021, pp 1-21.

[5] *G.G. Wang, I. Horowitz, S.H. Wang and C.W. Chen.* "A control design for a tracked vehicle with implicit nonlinearities using quantitative feedback theory"// IEEE Conference on Decision and Control. IEEE, December. **vol. 3**, 1988 pp. 2416-2418.

[6] *B. Cao; M. G. Brandon, X. Wang, Y. Zou, G. F. Reed and Z. H. Mao*. "Direct torque model predictive control of a five-phase permanent magnet synchronous motor". IEEE Transactions on Power Electronics, **vol. 36**, no. 2 July. 2020, pp. 2346-2360.

[7] *S. Niu, Y. Luo, W. Fu and X. Zhang* "Robust model predictive control for a three-phase PMSM motor with improved control precision". IEEE Transactions on Industrial Electronics, **vol. 68**, no. 1 August. 2020, pp. 838-849.

[8] *F. C. Sun and S. Y. Chen*. "Matching theory of induction motor drive system for tracked vehicles". Journal of Mechanical Engineering, **vol. 44**, no. 11 2008 pp. 260-266.

[9] *C. Attaianese, M. Di Monaco, I. Spina, and T. Giuseppe*. "A variational approach to MTPA control of induction motor for EVs range optimization". IEEE Transactions on Vehicular Technology, **vol. 69**, no. 7 March 2020, pp. 7014-7025.

[10] *S. Y. Chen and F. C. Sun*. "Modeling and performance prediction of induction motor drive systems for electrically driven tracked vehicles". Journal of Military Engineering **vol. 04**, 2006 pp. 592-597.

[11] *X. Xiao, Y. Yan and B. Chen*. "Stochastic dynamic analysis for vehicle-track-bridge system based on probability density evolution method". Engineering Structures, **vol. 188**, no. 1 June 2019, pp. 745-761.

[12] *E. Aggestam and J C Nielsen*. "Simulation of vertical dynamic vehicle–track interaction using a three-dimensional slab track model". Engineering Structures, **vol. 222**, no. 1 November 2020.

[13] *Z. Zhan, G. Si, J. Zhi and L. Liu* "Design and analysis based on RecurDyn of the electric crawler type remote controlled hedge trimmer"//Journal of Physics: Conference Series. IOP Publishing, **vol. 1633**, no. 1. May. 2020.

[14] *H. Y. Wang, Q. L. Wang and Q*. Rui. "Analysis and experimental verification of steering process of high-speed tracked vehicles". Journal of Mechanical Engineering, **vol. 50**, no. 16 2014, pp. 162-172.

[15] *J. T. Gai, C. S. Liu and C. J. Ma.* "Steering control of electrically driven tracked vehicles considering track slip and slide". Journal of Military Engineering, **vol. 42**, no. 10. pp. 2092-2101.

[16] *S. Y. Chen, F. C. Sun and C. N. Zhang*. "Co-simulation and experimental research on the dynamic performance of electrically driven tracked vehicles". Journal of System Simulation, **vol. 06**, 2007 pp. 1370-1375.

[17] *Y. Chi, H. T. Wang and D. D. Shi*. "Study on the load ratio of sliding turn in small radius differential steering of tracked vehicles". Journal of Northeast Agricultural University, **vol. 45**, no. 12. 2014 pp. 112-118.

[18] *K. F. Fu.* "Research on key parameters matching and energy management of CVT-equipped PHEVs". Chongqing University, 2015 pp. 10-22.

[19] *Y. Jiang, Z. Wang and C. Tian.* "A method for matching motor parameters of 565kW electric drive crawler bulldozer". Southern Agricultural Machinery, **vol. 51**, no. 11. 2020 pp. 109-110.

[20] *K. Song and T. Zhang*. "Parameter matching of electric motor drive trains for pure electric and series hybrid vehicles". Automotive Engineering, **vol. 35**, no. 06. 2013 pp. 559-564.